

Mechanism-Based Modeling of Tumor Growth and Treatment Response Constrained by Multiparametric Imaging Data

David A. Hormuth II, PhD¹; Angela M. Jarrett, PhD¹; Ernesto A.B.F. Lima, PhD¹; Matthew T. McKenna, PhD²; David T. Fuentes, PhD³; and Thomas E. Yankeelov, PhD¹

Multiparametric imaging is a critical tool in the noninvasive study and assessment of cancer. Imaging methods have evolved over the past several decades to provide quantitative measures of tumor and healthy tissue characteristics related to, for example, cell number, blood volume fraction, blood flow, hypoxia, and metabolism. Mechanistic models of tumor growth also have matured to a point where the incorporation of patient-specific measures could provide clinically relevant predictions of tumor growth and response. In this review, we identify and discuss approaches that use multiparametric imaging data, including diffusion-weighted magnetic resonance imaging, dynamic contrast-enhanced magnetic resonance imaging, diffusion tensor imaging, contrast-enhanced computed tomography, [¹⁸F]fluorodeoxyglucose positron emission tomography, and [¹⁸F]fluoromisonidazole positron emission tomography to initialize and calibrate mechanistic models of tumor growth and response. We focus the discussion on brain and breast cancers; however, we also identify three emerging areas of application in kidney, pancreatic, and lung cancers. We conclude with a discussion of the future directions for incorporating multiparametric imaging data and mechanistic modeling into clinical decision making for patients with cancer.

Clin Cancer Inform. © 2019 by American Society of Clinical Oncology

INTRODUCTION

Medical imaging plays a critical role in the assessment and diagnosis of solid tumors. After diagnosis, a series of imaging data are collected to evaluate tumor size, invasion into adjacent structures, and metastatic spread. These data are used in conjunction with a clinical staging model to help to guide treatment decisions and provide a crude prognosis for the disease course. A current challenge in clinical oncology is to predict the response of the individual patient to a specified therapeutic approach. Although the aforementioned measures can provide a general prognosis that is based on the stage of the disease and historical data, the specific response of the patient population to standard therapies is heterogeneous. A potential approach to this challenge is to leverage radiographic changes, which can readily be acquired at multiple time points before and during therapy, to enable patient-specific predictions of treatment response.

The radiographic assessment of changes in tumor size after treatment has been standardized to categorize treatment response objectively. One commonly used technique is the Response Evaluation Criteria in Solid Tumors (RECIST).^{1,2} RECIST primarily relies on morphologic changes to identify patient response. However, the predictive utility of these measures is fundamentally limited because the morphologic

changes that form the basis of RECIST are temporally downstream of the underlying biochemical responses to therapy. Developments in imaging technologies have moved well beyond morphologic characterization and can provide noninvasive characterization of the tumor microenvironment.³ Post-treatment changes in magnetic resonance imaging (MRI) or positron emission tomography (PET) measures of hypoxia,⁴ cellularity,^{5,6} blood volume,⁷ and perfusion^{8,9} may be predictive of response. The incorporation of these advanced imaging measures into mechanism-based models presents an opportunity to fundamentally shift cancer care through the development of individually optimized therapies.^{10,11} Of note, mechanism-based mathematical models of disease represent a fundamentally different approach to relying only on statistical data analysis (big data). This approach does not dispute that statistical inference in itself is not of critical importance; rather, by its very nature, it is based on statistical properties of large populations of patients in which conditions that prevail in specific individuals are hard to detect. That is, the big data–only approach captures the general trends but cannot account for subtle changes in the individual patient (the very characteristics that make us individuals) over an extended time. Imaging-based mechanistic models are designed to predict the spatiotemporal changes associated with disease onset, progression, and

Author affiliations and support information (if applicable) appear at the end of this article.

Accepted on July 5, 2018 and published at ascopubs.org/journal/cci on February 26, 2019; DOI <https://doi.org/10.1200/CCI.18.00055>

response to therapy. Such a validated mathematical framework enables the generation of testable, patient-specific hypotheses *in silico*, thereby allowing optimization of interventions for the individual patient by using the specific characteristics of the patient's unique situation.

Mechanism-based models are built on the assumption that behavior of a complex system can be predicted with mathematical descriptions of the interactions of individual system components. Only recently have these models begun to incorporate noninvasive imaging measurements^{12,13} as a means to parameterize these models on a patient-specific basis. Noninvasive imaging techniques are well suited for model initialization and calibration because they can provide repeatable, reproducible, and evenly discretized measures of tumor properties before, during, and after therapy. The initialization and calibration mechanism-based models of tumor growth on an individual basis facilitate the generation of individual forecasts of response to chemotherapies,^{14,15} radiation therapy (RT),^{11,16,17} and resection¹⁸ that could be used for therapeutic planning. One potential (clinical) utility of mechanism-based models is in the application of optimized and adaptive RT plans. RT is a central component of the standard of care for many cancers, with medical imaging playing a critical role in the positioning and guidance of RT.¹⁹ Adaptive RT is a strategy to alter treatment plans and delivery to control for variations in patient radiosensitivity.²⁰ One potential scenario for mechanistic modeling is to use patient data before and during therapy to calibrate predictive models of tumor growth and response to determine a patient's response to therapy. Guided by model predictions, clinicians could simulate alternative treatment plans and select a plan that improves the patient's outcome. This modeling scenario could then be repeated every time new data are collected to provide a means to continuously adapt therapy for individual patients. Recent developments in MRI-guided linear accelerators²¹ could be used to provide the necessary quantitative multiparametric data to update model calibrations and adapt patient therapy.

Two barriers to implementing imaging-based mechanistic modeling are the access to proper data and the validity of current mathematical descriptions of tumor growth and response. In this review, we identify the type of data imaging measures can provide and proceed to the numerical methods, considerations required for implementation and validation. We then present current modeling approaches with examples from cancer of the brain, breast, pancreas, kidney, and lung. Finally, we identify future opportunities in this emerging subfield of oncology frequently referred to as mathematical oncology.²²

IMAGING MEASUREMENTS AND PATIENT DATA

Multiparametric Imaging Measures of Tumor and Tissue Properties

This section identifies some of the imaging techniques that currently are being used in mechanistic models of tumor

growth. Tumor cellularity (or the number of cells within an imaging voxel) can be estimated by using diffusion-weighted MRI²³ (DW-MRI), dynamic contrast-enhanced MRI^{24,25} (DCE-MRI), and contrast-enhanced computed tomography^{26,27} (CE-CT). A variant of DW-MRI called diffusion tensor imaging²⁸ (DTI) also can be used to assess the magnitude and direction of water diffusion in tissue, thereby providing an estimate of the preferred direction of tumor cell movement. Properties of the tumor vasculature, such as blood volume and perfusion, can be estimated by using contrast-based techniques, such as DCE-MRI²⁴ and dynamic CE-CT.²⁶

Several PET tracers have been developed that can provide estimates of glucose uptake, tumor hypoxia, and cell proliferation. [¹⁸F]-fluorodeoxyglucose²⁹ (¹⁸FDG) is a glucose analog that is taken up by cells, phosphorylated, and then trapped within the cell; thus, FDG preferentially accumulates within metabolically active cells. [¹⁸F]Fluoromisonidazole³⁰ (¹⁸F-MISO) is a PET tracer commonly used to assess the level of hypoxia in tumors. A summary of the measurable quantities discussed in this section is listed in Table 1, whereas Figure 1 shows an example of quantitative PET and MRI data acquired in a patient with breast cancer before and after the start of therapy.

Challenges in the Acquisition, Processing, and Sharing of Patient Image Data

Although multiparametric imaging data are the focus of this review, many pieces of information are needed to provide informative model predictions to clinicians. This section highlights challenges and concerns about imaging metadata, medical records, instrument types and variability, and data sharing. A more comprehensive review of these challenges can be found in Yankeelov et al³¹ and Shaikh et al.³²

Imaging metadata (eg, observations, tissue annotations) and medical records are essential for the proper use of imaging data sets. These data often are stored separately from the image data themselves and require database management³³ to connect metadata and medical records

TABLE 1. Summary of Tumor Properties Available From Common Medical Imaging Techniques

Property	Modality
Cellularity	DW-MRI, ²³ DCE-MRI, ²⁴ CE-CT ²⁶
Direction of cell movement	DTI ²⁸
Blood volume and perfusion	DCE-MRI, CE-CT
Hypoxia or hypoxic tissues	¹⁸ F-MISO-PET ³⁰
Glucose metabolism	¹⁸ FDG-PET ²⁹

Abbreviations: CE-CT, contrast-enhanced computed tomography; DCE-MRI, dynamic contrast-enhanced magnetic resonance imaging; DTI, diffusion tensor imaging; DW-MRI, diffusion-weighted magnetic resonance imaging; ¹⁸FDG, [¹⁸F]fluorodeoxyglucose; ¹⁸F-MISO, [¹⁸F]fluoromisonidazole; PET, positron emission tomography.

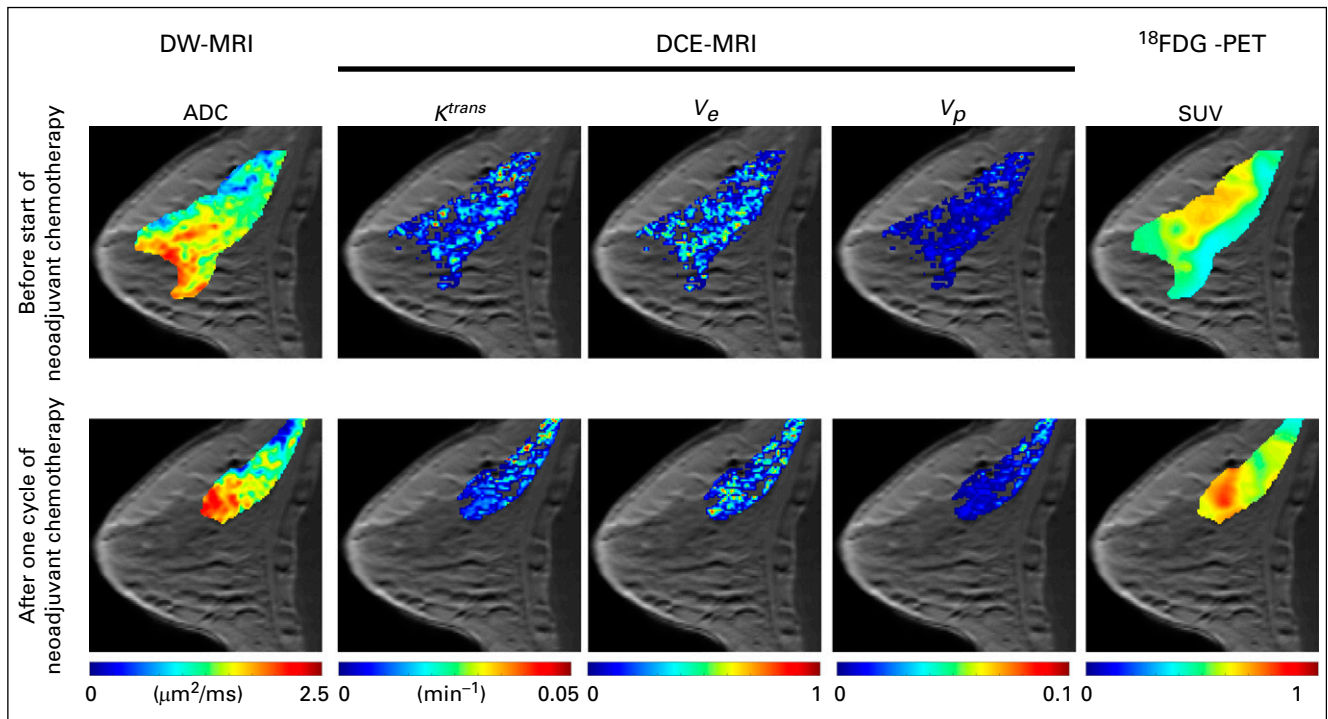


FIG 1. Example multiparametric data acquired in a patient with breast cancer before and after one cycle of neoadjuvant chemotherapy. Diffusion-weighted magnetic resonance imaging (DW-MRI) returns estimates of the apparent diffusion coefficient (ADC), which can be used to provide estimates of cellularity. Dynamic contrast-enhanced MRI (DCE-MRI) provides estimates of tissue blood flow and permeability (K^{trans}), extracellular-extravascular volume fraction (v_e), and plasma volume fraction (v_p). [^{18}F]Fluorodeoxyglucose positron emission tomography (^{18}F FDG-PET) provides estimates of the glucose standardized uptake value (SUV). These imaging measurements can be acquired noninvasively before, during, and after the start of therapy to characterize functional changes in tumor properties.

to the appropriate image series. Modelers should be aware of medical details (eg, patient's individual history, disease subtypes, treatment schedules,³⁴ response) to model treatment response accurately. When sharing data, researchers should use consistent file types, naming procedures, and de-identification procedures to ease the interpretation and use of imaging data. Curated repositories³⁵ can provide a mechanism for archived data to meet consistent standards and improve the utility of shared data.

Site-to-site variation in image acquisition and analysis also may affect the interpretation of imaging data. Researchers should establish the repeatability and reproducibility of the imaging techniques used in their study.³¹ In addition, postprocessing (eg, tissue segmentation, image analysis) procedures should be reproducible within and outside a site to provide consistent analysis of the imaging data.³⁴ These analyses are particularly important when working with data acquired from multiple institutions with different instruments and different postprocessing routines.³⁶⁻⁴⁰

NUMERICAL METHODS

This section reviews the calibration, selection, and validation of models; the sensitivity analysis of the parameters; and how to address uncertainties in data, model selection, parameter estimation, and predictions. Figure 2 shows

a schematic of a framework for model calibration, selection, and validation.

Model Calibration, Selection, and Validation

For a given problem (eg, the prediction of tumor growth^{41,42}), different mathematical models can be developed on the basis of the hypotheses to be tested. This will lead to different sets of parameters within the model that need to be estimated. The process of determining the values of the free parameters within a model is called calibration, and it frequently involves the solving of an inverse problem for the parameters that are based on experimental observations. More specifically, for a given model $M(\psi)$, where ψ represents the model parameters, calibration consists of minimizing the residual $R = y - M(\psi)$, where y is the measured data.⁴³⁻⁴⁵ If the parameters are properly calibrated, then $R = 0$, assuming that no experimental error or model inadequacy exists.⁴⁶ This minimization process can be done in a deterministic or statistical framework. The deterministic framework searches for the set of parameter values that minimize the residual error. In the statistical framework, the parameters are assumed to have a prior distribution that contains the true parameter. The statistical model is the probability distribution image of the mechanistic model applied to the prior distribution. The data are just one realization of this model.⁴⁴ Through Bayes' theorem, the data

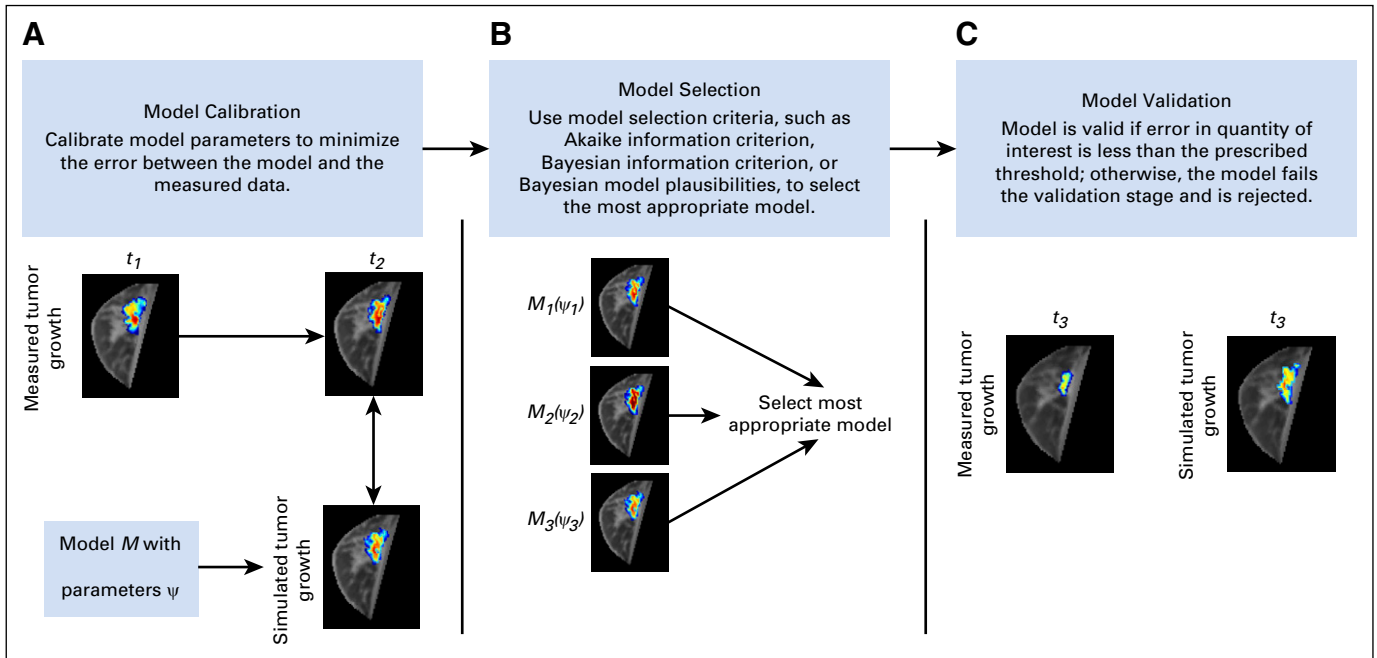


FIG 2. Schematic of model calibration, selection, and validation framework. (A) A deterministic or statistical approach to model calibration is used to minimize the error between the model and the measurement of a specific quantity of interest (eg, tumor volume, cell density distribution). In this example, the model is initialized at time point 1 (t_1), and the error is calculated at time point 2 (t_2). (B) Model selection criteria are used to select the most appropriate model that accurately describes the data. (C) The selected model is then evaluated in a validation stage by simulating tumor growth at time point 3 (t_3) and comparing it with the measured tumor growth. If the model error is within a prescribed error threshold for a quantity of interest, it is considered valid.

are used to improve knowledge with regard to the parameter distribution. Among the enormous number of possible calibrated models, selection of which model is the best for predicting the quantities of interest is crucial. Two common methods are based on information theory, such as the Akaike information criterion⁴⁷ and the Bayesian information criterion,⁴⁸ that penalizes the number of parameters from the model. After the best model is selected, whether the model is capable of predicting the quantities of interest with sufficient accuracy must be determined. This process is called validation and involves experimental observations obtained from more-complex scenarios than those involved in the calibration process or an independent subset of the data not used during the calibration step. The model is tested at this new scenario with the calibrated parameters, and if the differences between the values of quantities of interest is less than the (user-defined) tolerance, the model is valid; however, technically, one can only say that with this metric and with this tolerance, the model is not invalid because additional information always could falsify a model. Thus, a not informative or inaccurate model is invalid because it does not satisfy the validation metric that compares the model prediction with experimental data.⁴⁶

Sensitivity Analysis

Sensitivity analysis refers to quantitatively understanding how variation in a model's parameters influences the output of the model. (This is not to be confused with uncertainty

analysis, which generally refers to a lack of knowledge about parameter values.) The goal of a sensitivity analysis is to rank parameters by their importance on the basis of how their prescribed variations affect the output measures compared with the results from other parameters' changes. This provides a means to identify the driving interactions of the system and narrow the scope for which parameters should be targeted for experimental estimation (which is particularly useful for complex systems) or to identify parameters that could be eliminated or set to a nominal value. A broad range of methods for calculating sensitivity measures can be divided into two major groups: local and global. For local sensitivity measures, each parameter is varied individually, whereas for global sensitivity measures, individual parameter sensitivity is determined while all parameters are varied. Although global methods are more computationally expensive, they are less likely to miscategorize an important parameter as insignificant. Within these two groups, the types of analyses range from derivatives that determine local dependence,^{49,50} statistical methods that use correlations,⁵¹⁻⁵³ popular variance-based methods,⁵⁴⁻⁵⁸ and even methods that consider the shape of output distributions.^{59,60} Careful examination of individual sensitivity methods should be performed before choosing a sensitivity index to rank parameters in a model because different methods can give differing rankings of parameters or can even disagree on the importance of particular parameters overall.

Uncertainty Quantification

The construction of models to represent most phenomena are subject to uncertainties in the observational data parameters and in the mathematical and computational models (eg, model structure, modeling assumptions, constitutive laws, boundary conditions). The models can be subject to epistemic uncertainties because of our lack of knowledge about the parameters or aleatoric uncertainties because of the parameter variability.⁶¹ Disregard of such uncertainties would lead to biased predictions of the quantities of interest. In particular, for the tumor growth models, uncertainty can lead to under- or overestimation of the tumor size/position or incorrect treatment protocols and might lead to selection of an inadequate model.⁶² To have a way to quantify these uncertainties and their propagation through the several steps that lead to model prediction is of fundamental importance. One way is through Bayesian approaches where the parameters, the data, and the model are not assumed to be deterministic and, instead, are considered as random variables characterized by probability density functions.⁶³ These characterizations lead to a stochastic model able to propagate uncertainty from model inputs to outputs.

EXAMPLES FROM THE LITERATURE

Brain Cancer

Mathematical modeling of glioblastoma using advanced imaging techniques to initialize and calibrate subject-specific models of growth and response to therapy is well developed in the literature.^{16-18,64-71} Tumor growth in general and glioblastoma growth in particular commonly have been modeled using a reaction-diffusion-type model that describes the proliferation (reaction) and movement (diffusion) of tumor cells, as shown in Equation 1:

$$\frac{\partial N(\bar{x}, t)}{\partial t} = \overbrace{\nabla \cdot [D \nabla N(\bar{x}, t)]}^{\text{Diffusion}} + \overbrace{k \cdot N(\bar{x}, t) \left(1 - \frac{N(\bar{x}, t)}{\theta} \right)}^{\text{Proliferation}} \quad (1)$$

where $N(\bar{x}, t)$ is the number of tumor cells at a given three-dimensional position \bar{x} and time t , D is the tumor cell diffusion coefficient, k is the proliferation rate, and θ is the carrying capacity or the maximum number of cells that can be fit within a volume of interest (eg, a voxel). Baldock et al⁶⁵ pioneered image-based model calibration for glioblastoma by introducing the use of anatomic T_1 - and T_2 -weighted MRI to provide estimates of the detectable tumor and the infiltrative nondetectable tumor margins, respectively. Model parameters calibrated from individual patients through this approach correlated with tumor grade,⁷² overall patient survival,⁷³ and prediction of response to therapy.^{16,18} This approach has been expanded by many groups to include multiparametric imaging measures from MRI^{17,70,71,74,75} and PET.⁶⁶ The incorporation DTI data has been investigated as a means to introduce anisotropic movement of tumor cells.^{67-70,74-76} It has been suggested

that the direction of cell movement is aligned with the diffusion tensor direction,⁷⁰ which potentially introduces anisotropic cell diffusion within the brain. DTI data often are incorporated in mechanistic models that use data acquired in the individual patient^{68,74,75} or supplied from a common brain atlas.^{67,69,70,76} In Swan et al,⁷⁴ the incorporation of anisotropic diffusion (by using DTI data) compared with isotropic diffusion showed promising results, where a higher level of overlap between the model and measured tumor volumes was observed for the anisotropic diffusion model for nine of the 10 patients observed. This approach potentially could be used to identify infiltrative regions or define treatment volumes that incorporate areas where tumor cells are likely to migrate. ¹⁸F-MISO-PET data also have been incorporated into a reaction-diffusion-type model of response to RT.⁶⁶ The level of hypoxia as assessed from ¹⁸F-MISO uptake was used to assign an oxygen-enhancing ratio to spatially vary the radiosensitivity of tumor cells to the delivered therapy. Rockne et al⁶⁶ observed in one patient data set that incorporation of ¹⁸F-MISO data in their mechanistic model relative to the model that did not include ¹⁸F-MISO decreased the error in tumor volume predictions from 14.6% to 1.1%. Several efforts have proposed the incorporation of DW-MRI estimates of cellularity,^{17,64,71} fluid-attenuated inversion recovery MRI estimates of edema,⁷⁷ DCE-MRI estimates of perfusion,⁷⁷ and DCE-MRI estimates of blood volume fraction.⁷⁸

Breast Cancer

Imaging-based models for breast cancer have been developing quickly over the past decade, beginning first with DW-MRI measures used to approximate tumor cell number and initialize a simple logistic growth model (ie, tumor cell proliferation slows as it reaches a carrying capacity) to predict tumor growth.⁷⁹ By using DW-MRI data for individual patients, the tumor cell number within the tumor region of interest was estimated from the apparent diffusion coefficient value. For each patient, one pretreatment scan and one early post-treatment scan were used to calibrate the parameters of the model, which were then used to simulate the tumor forward to be compared with the third imaging time point. By using these patient-specific data, the mathematical model's prediction for tumor cell numbers in the patient's third scan was found to be statistically correlated to the corresponding experimental data. Later, DW-MRI data were used to initialize a partial differential equation model that included a mathematical diffusion term to simulate the outward movement of cells as the tumor mass grows (mass effect) on the basis of similar modeling efforts for glioblastomas.⁸⁰ The mechanical properties of these different tissues were incorporated by modulating the diffusive effect of the tumor cells. Briefly, this coupled model describes tumor growth changes that can cause deformations in the surrounding healthy tissues and potentially increase stress and therefore reduce the

outward expansion of tumor growth.^{14,15,81} When compared with RECIST measures of response, the approach by Weis et al⁸¹ had increased specificity and equal sensitivity to RECIST results. The most recent work in this effort used DCE-MRI data to estimate the delivery of chemotherapy to the tumor. By using parameters derived from the extended Tofts-Kety²⁴ model built to determine the concentration of contrast agent in tissues for DCE-MRI, the concentration of drug in the tissue is approximated for each individual patient per voxel. The system of equations in Equation 2 are thus extended as follows (Equations 3 to 5):

$$\frac{\partial N(\bar{x}, t)}{\partial t} = \frac{\text{Diffusion}}{\nabla \cdot [D \nabla N(\bar{x}, t)]} + \frac{\text{Proliferation}}{k \cdot N(\bar{x}, t) \left(1 - \frac{N(\bar{x}, t)}{\theta}\right)} - \frac{\text{Drug delivery}}{\alpha C_{\text{tissue}}^{\text{drug}}(\bar{x}, t) N(\bar{x}, t)} \quad (2)$$

$$C_{\text{tissue}}^{\text{drug}}(\bar{x}, t) = \frac{\text{Extracellular extravascular compartment}}{K^{\text{trans}}(\bar{x}) \int_0^t \left[C_{\text{plasma}}^{\text{drug}}(u) \cdot \exp\left[-\frac{K^{\text{trans}}(\bar{x})}{v_e(\bar{x})}(t-u)\right] \right] du} + \frac{\text{Vasculature compartment}}{v_p(\bar{x}) C_{\text{plasma}}^{\text{drug}}(t)} \quad (3)$$

$$D(\bar{x}, t) = D_0 \exp[-\gamma \sigma_{vm}(\bar{x}, t)] \quad (4)$$

$$\frac{\text{Linear elastic model for tissue displacement}}{\nabla \cdot G \nabla \bar{u}} + \nabla \left[\frac{G}{1-2\nu} \nabla \bar{u} \right] - \frac{\text{Local body force from invading tumor}}{\lambda \nabla \bar{N}(x, t)} = 0 \quad (5)$$

where $N(\bar{x}, t)$ is the number of tumor cells at time t , D is the diffusion coefficient, $k(\bar{x})$ is a spatially resolved proliferation rate map for tumor cells, θ is the carrying capacity, and $C_{\text{tissue}}^{\text{drug}}(\bar{x}, t)$ is the approximate amount of drug therapy in the tissue at time t with effectiveness α . K^{trans} is the volume transfer constant from the plasma space to the tissue space, v_p is the volume fraction of the plasma space, and v_e is the volume fraction of the extravascular extracellular space²⁴ and $C_{\text{plasma}}^{\text{drug}}(t)$ is the concentration of the drug in the plasma. D_0 is the tumor cell diffusion constant in the absence of stress; γ is an empirical coupling constant for the von Mises stress σ_{vm} ; G is the shear modulus, where $G = E / [2(1 - \nu)]$ for the Young's modulus (E) and Poisson ratio (ν) material properties; \bar{u} is the displacement as a result of tumor cell growth; and λ is another empirical coupling constant. (σ_{vm} reflects the experienced stress and often is used within failure criterion strategies in materials.) Preliminary results in a cohort of five patients showed reductions in the error between the model's predictions of tumor cellularity and size compared with when drug therapy is not incorporated explicitly. This approach demonstrates the plausibility of

using DCE-MRI to characterize drug delivery and represents a step toward the goal of achieving a patient-specific model for predicting tumor response to neoadjuvant chemotherapy in breast cancer.⁸²

Other Disease Sites

The mathematical modeling frameworks developed for glioblastoma and breast cancer have, in principle, application to any solid tumor type. Recently, image-based models also have been developed for kidney,⁸³ lung,⁸⁴ and pancreatic⁸⁵ tumors. For example, Chen et al^{83,86} leveraged CE-CT images to develop a reaction-diffusion equation to predict kidney tumor growth on a longitudinal image series, which expanded Equation 1 to include a biomechanical model that related tumor cell density to a force applied on the surrounding tissue. In this effort, Chen et al observed an average error in tumor volume predictions of 5.1% in five patients. Mi et al⁸⁴ developed an advection-reaction model of lung tumor growth during RT that leveraged PET/CT imaging. Tumor cell diffusion was assumed to be negligible within the lung, and any motion (the advection term) was assumed to be the result of cells migrating toward increased concentrations of oxygen, nutrients, and space. The group assumed cell density to be proportional to the ¹⁸F-FDG-PET standardized uptake value, and the model provided a means to estimate the effect of radiotherapy. The approach demonstrated promising results in a cohort of seven patients with non-small-cell lung carcinoma, with an average concordance of 76% between measured and predicted tumor volumes. The group extended this approach to improve tumor segmentation on subsequent imaging data, which provided a method to estimate more accurately tumor changes (and thus model parameters), and thereby, to improve model predictions of tumor volumes.⁸⁷ Liu et al⁸⁵ developed a reaction-advection-diffusion model to describe the proliferation of tumor cells (reaction), the movement of tumor cells to displacement (advection), and the movement of tumor cells as a result of diffusion to predict the growth of pancreatic tumors. The model was parameterized by using ¹⁸F-FDG-PET and dual-phase CT to estimate the proliferation rate and cellular volume fraction, respectively. The model of Liu et al was expanded recently by modeling tumor mass effects with elastic growth decomposition, which separates the continuous deformation field of a growing tumor into its elastic and growth components to describe more accurately pancreatic tumor behavior.²⁷ These examples demonstrate the broad application areas for image-based models of cancer growth and treatment response.

FUTURE DIRECTIONS

There are two fundamental barriers to the field of imaging-based mechanistic modeling of tumor growth and response to treatment being able to reach its promise: access to proper data and model validity. Mechanism-based models require a level of quantification that is not

typically available in the standard-of-care setting. The majority of imaging data types acquired as standard of care are limited to qualitative descriptions of tissue morphology. Such data types fundamentally limit the calibration and prediction fidelity that can be achieved with mechanism-based models. Thus, specialized clinical studies must be designed and executed to provide the data types needed to initialize and constrain these models. With such data available, systematic testing of the validity of a range of mathematical models that account for a wide range of biologic and physical factors becomes possible, which leads to an entire family of potentially predictive models. Model selection algorithms then can be used to select the optimal model and validate its ability to accurately predict the spatiotemporal development of an individual patient's tumor.^{41,42}

If these two limitations can be overcome, or even partially addressed, then it may be possible to build, calibrate, and apply realistic mathematical models for use in patient care. Figure 3 shows a schematic diagram for how such an

approach could be realized. Initially, a mathematical formulation is defined to model the desired quantity of interest. In vitro experiments can be used to acquire knowledge on parameter values⁴³ (Fig 3A). Imaging data are then acquired before, during, and early in the course of therapy (Fig 3B). The images are spatially coregistered (or aligned) across time, discretized, and segmented according to the important features to be captured by the model. The values of the parameters are updated on this patient-specific scenario. With the optimized parameter values, the model passes through the validation step (Fig 3C). If deemed valid, the model can be used with some confidence to make a prediction. This prediction will provide additional scores or model-based biomarkers to be used to improve current clinical staging models and response assessment criteria or to define new therapy protocols. Success in this program would represent, without question, an enormous improvement in the human condition.

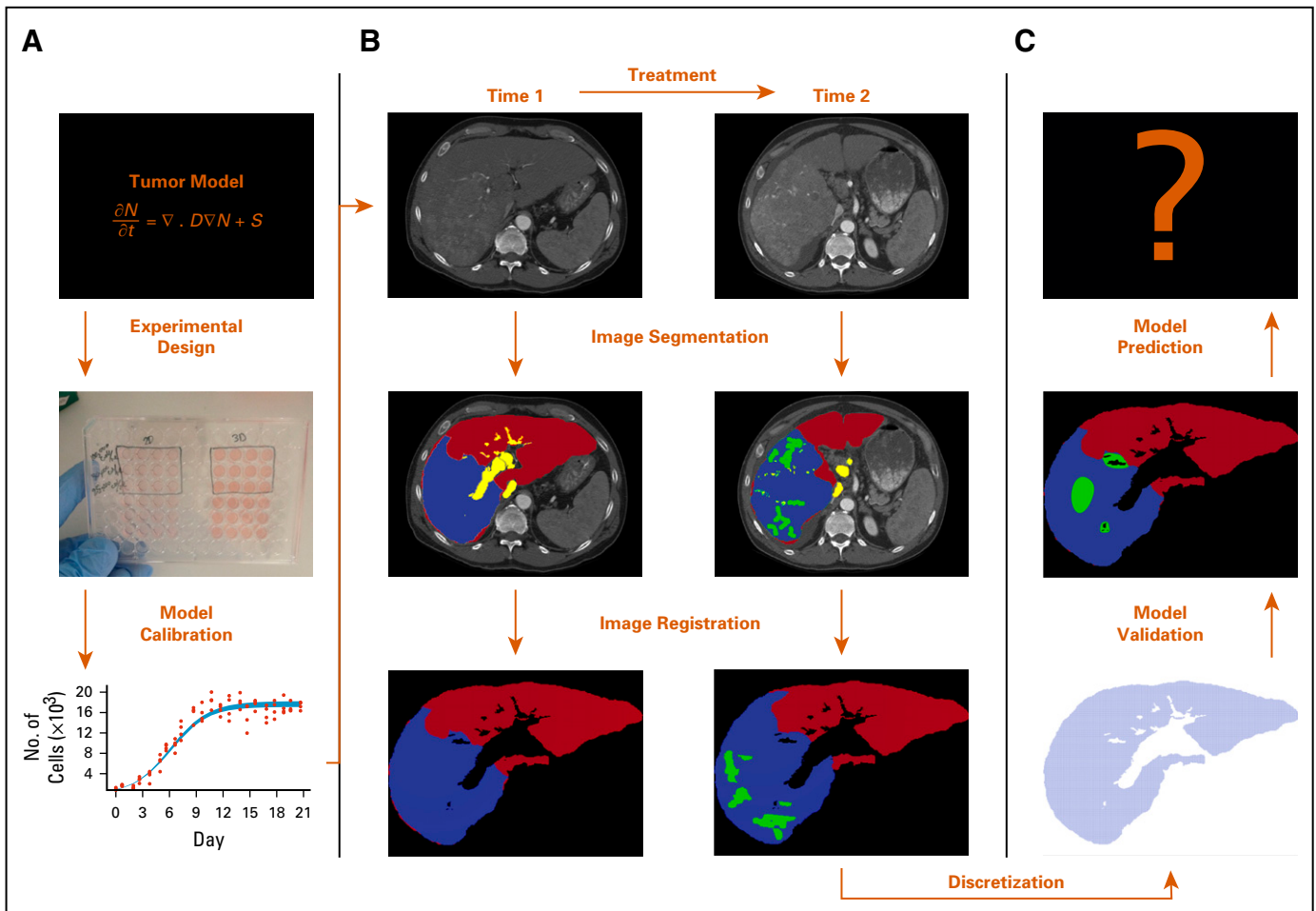


FIG 3. Modeling framework that describes how a mathematical model can be developed and implemented. (A) In vitro experiments provide data to calibrate a particular tumor model. (B) Triphase computed tomography data are acquired (before and after treatment), segmented, and registered. (C) The domain is discretized so that the model can be calibrated and validated to patient data. If the model meets validation criteria, it can be used to predict tumor evolution.

In summary, the integration of mechanism-based mathematical modeling with quantitative, multiparametric imaging data that capture the unique characteristics of the individual patient promises to generate accurate and

actionable predictions that can optimally guide the care of the patient. This would fundamentally shift existing paradigms of therapy monitoring and selection in cancer and hasten personalized cancer medicine.

AFFILIATIONS

¹The University of Texas at Austin, Austin, TX

²Vanderbilt University, Nashville, TN

³The University of Texas MD Anderson Cancer Center, Houston, TX

CORRESPONDING AUTHOR

Thomas E. Yankeelov, PhD, Department of Biomedical Engineering, The University of Texas at Austin, 107 W Dean Keeton St, Stop C0800, Austin, TX 78712; e-mail: thomas.yankeelov@utexas.edu.

SUPPORT

Supported by National Cancer Institute Grant No. U01 CA174706 and U01 CA154602 and Cancer Prevention Research Institute of Texas Grant No. RR160005.

AUTHOR CONTRIBUTIONS

Conception and design: David A. Hormuth II, Angela M. Jarrett, Matthew T. McKenna, Thomas E. Yankeelov

Collection and assembly of data: Matthew T. McKenna, Thomas E. Yankeelov

Data analysis and interpretation: David A. Hormuth II, Ernesto A.B.F. Lima, David T. Fuentes, Thomas E. Yankeelov

Manuscript writing: All authors

Final approval of manuscript: All authors

Accountable for all aspects of the work: All authors

AUTHORS' DISCLOSURES OF POTENTIAL CONFLICTS OF INTEREST

The following represents disclosure information provided by authors of this manuscript. All relationships are considered compensated.

Relationships are self-held unless noted. I = Immediate Family Member, Inst = My Institution. Relationships may not relate to the subject matter of this manuscript. For more information about ASCO's conflict of interest policy, please refer to www.asco.org/rwc or ascopubs.org/jco/site/ifc.

No potential conflicts of interest were reported.

REFERENCES

1. Therasse P, Arbuuck SG, Eisenhauer EA, et al: New guidelines to evaluate the response to treatment in solid tumors. European Organization for Research and Treatment of Cancer, National Cancer Institute of the United States, National Cancer Institute of Canada. *J Natl Cancer Inst* 92:205-216, 2000
2. Eisenhauer EA, Therasse P, Bogaerts J, et al: New Response Evaluation Criteria in Solid Tumours: Revised RECIST guideline (version 1.1). *Eur J Cancer* 45:228-247, 2009
3. Yankeelov TE, Abramson RG, Quarles CC: Quantitative multimodality imaging in cancer research and therapy. *Nat Rev Clin Oncol* 11:670-680, 2014
4. Sorace AG, Syed AK, Barnes SL, et al: Quantitative [¹⁸F]FMISO PET imaging shows reduction of hypoxia following trastuzumab in a murine model of HER2+ breast cancer. *Mol Imaging Biol* 19:130-137, 2017
5. Schmainda KM: Diffusion-weighted MRI as a biomarker for treatment response in glioma. *CNS Oncol* 1:169-180, 2012
6. Padhani AR, Liu G, Koh DM, et al: Diffusion-weighted magnetic resonance imaging as a cancer biomarker: Consensus and recommendations. *Neoplasia* 11:102-125, 2009
7. Galbán CJ, Chenevert TL, Meyer CR, et al: Prospective analysis of parametric response map-derived MRI biomarkers: Identification of early and distinct glioma response patterns not predicted by standard radiographic assessment. *Clin Cancer Res* 17:4751-4760, 2011
8. Virostko J, Hainline A, Kang H, et al: Dynamic contrast-enhanced magnetic resonance imaging and diffusion-weighted magnetic resonance imaging for predicting the response of locally advanced breast cancer to neoadjuvant therapy: A meta-analysis. *J Med Imaging (Bellingham)* 5:011011, 2018
9. Barnes SL, Sorace AG, Whisenant JG, et al: DCE- and DW-MRI as early imaging biomarkers of treatment response in a preclinical model of triple negative breast cancer. *NMR Biomed* 30:3799, 2017
10. Yankeelov TE, Quaranta V, Evans KJ, et al: Toward a science of tumor forecasting for clinical oncology. *Cancer Res* 75:918-923, 2015
11. Corwin D, Holdsworth C, Rockne RC, et al: Toward patient-specific, biologically optimized radiation therapy plans for the treatment of glioblastoma. *PLoS One* 8:e79115, 2013
12. Yankeelov TE, Atuegwu N, Hormuth DA, et al: Clinically relevant modeling of tumor growth and treatment response. *Sci Transl Med* 5:187ps9, 2013
13. Atuegwu NC, Gore JC, Yankeelov TE: The integration of quantitative multi-modality imaging data into mathematical models of tumors. *Phys Med Biol* 55:2429-2449, 2010
14. Weis JA, Miga MI, Arlinghaus LR, et al: Predicting the response of breast cancer to neoadjuvant therapy using a mechanically coupled reaction-diffusion model. *Cancer Res* 75:4697-4707, 2015
15. Weis JA, Miga MI, Arlinghaus LR, et al: A mechanically coupled reaction-diffusion model for predicting the response of breast tumors to neoadjuvant chemotherapy. *Phys Med Biol* 58:5851-5866, 2013
16. Rockne R, Rockhill JK, Mrugala M, et al: Predicting the efficacy of radiotherapy in individual glioblastoma patients in vivo: A mathematical modeling approach. *Phys Med Biol* 55:3271-3285, 2010
17. Hormuth DA 2nd, Weis JA, Barnes SL, et al: Biophysical modeling of in vivo glioma response after whole-brain radiation therapy in a murine model of brain cancer. *Int J Radiat Oncol Biol Phys*, 100:1270-1279, 2018
18. Swanson KR, Rostomly RC, Alvord EC Jr: A mathematical modelling tool for predicting survival of individual patients following resection of glioblastoma: A proof of principle. *Br J Cancer* 98:113-119, 2008
19. Jaffray DA: Image-guided radiotherapy: From current concept to future perspectives. *Nat Rev Clin Oncol* 9:688-699, 2012
20. Yan D: Adaptive radiotherapy: Merging principle into clinical practice. *Semin Radiat Oncol* 20:79-83, 2010

21. Lagendijk JJW, Raaymakers BW, Raaijmakers AJE, et al: MRI/linac integration. *Radiother Oncol* 86:25-29, 2008
22. Anderson ARA, Quaranta V: Integrative mathematical oncology. *Nat Rev Cancer* 8:227-234, 2008
23. Koh DM, Collins DJ: Diffusion-weighted MRI in the body: Applications and challenges in oncology. *Am J Roentgenol* 188:1622-1635, 2007
24. Yankeelov TE, Gore JC: Dynamic contrast enhanced magnetic resonance imaging in oncology: Theory, data acquisition, analysis, and examples. *Curr Med Imaging Rev* 3:91-107, 2009
25. Atuegwu NC, Arlinghaus LR, Li X, et al: Parameterizing the logistic model of tumor growth by DW-MRI and DCE-MRI data to predict treatment response and changes in breast cancer cellularity during neoadjuvant chemotherapy. *Transl Oncol* 6:256-264, 2013
26. O'Connor JPB, Tofts PS, Miles KA, et al: Dynamic contrast-enhanced imaging techniques: CT and MRI. *Br J Radiol* 84:S112-S120, 2011
27. Wong KCL, Summers RM, Kebebew E, et al: Pancreatic tumor growth prediction with elastic-growth decomposition, image-derived motion, and FDM-FEM coupling. *IEEE Trans Med Imaging* 36:111-123, 2017
28. Sundgren PC, Dong Q, Gómez-Hassan D, et al: Diffusion tensor imaging of the brain: Review of clinical applications. *Neuroradiology* 46:339-350, 2004
29. Kubota K: From tumor biology to clinical PET: A review of positron emission tomography (PET) in oncology. *Ann Nucl Med* 15:471-486, 2001
30. Eschmann SM, Paulsen F, Bedeshem C, et al: Hypoxia-imaging with (18)F-misonidazole and PET: Changes of kinetics during radiotherapy of head-and-neck cancer. *Radiother Oncol* 83:406-410, 2007
31. Yankeelov TE, Mankoff DA, Schwartz LH, et al: Quantitative imaging in cancer clinical trials. *Clin Cancer Res* 22:284-290, 2016
32. Shaikh FA, Kolowitz BJ, Awan O, et al: Technical challenges in the clinical application of radiomics. *JCO Clin Cancer Inform* doi: 10.1200/CC.17.00004
33. Korenblum D, Rubin D, Napel S, et al: Managing biomedical image metadata for search and retrieval of similar images. *J Digit Imaging* 24:739-748, 2011
34. Kaufmann M, Hortobagyi GN, Goldhirsch A, et al: Recommendations from an international expert panel on the use of neoadjuvant (primary) systemic treatment of operable breast cancer: An update. *J Clin Oncol* 24:1940-1949, 2006
35. Prior F, Smith K, Sharma A, et al: The public cancer radiology imaging collections of The Cancer Imaging Archive. *Sci Data* 4:170124, 2017
36. Grech-Sollars M, Hales PW, Miyazaki K, et al: Multi-centre reproducibility of diffusion MRI parameters for clinical sequences in the brain. *NMR Biomed* 28:468-485, 2015
37. Chenevert TL, Malyarenko DI, Newitt D, et al: Errors in quantitative image analysis due to platform-dependent image scaling. *Transl Oncol* 7:65-71, 2014
38. Malyarenko DI, Wilmes LJ, Arlinghaus LR, et al: QIN DAWG validation of gradient nonlinearity bias correction workflow for quantitative diffusion-weighted imaging in multicenter trials. *Tomography* 2:396-405, 2016
39. Ger RB, Mohamed ASR, Awan MJ, et al: A multi-institutional comparison of dynamic contrast-enhanced magnetic resonance imaging parameter calculations. *Sci Rep* 7:11185, 2017
40. Sorace AG, Wu C, Barnes SL, et al: Repeatability, reproducibility, and accuracy of quantitative mri of the breast in the community radiology setting. *J Magn Reson Imaging* 48:695-707, 2018
41. Lima EABF, Oden JT, Hormuth DA II, et al: Selection, calibration, and validation of models of tumor growth. *Math Models Methods Appl Sci* 26:2341-2368, 2016
42. Lima EABF, Oden JT, Wohlmuth B, et al: Selection and validation of predictive models of radiation effects on tumor growth based on noninvasive imaging data. *Comput Methods Appl Mech Eng* 327:277-305, 2017
43. Stein S, Zhao R, Haeno H, et al: Mathematical modeling identifies optimum lapatinib dosing schedules for the treatment of glioblastoma patients. *PLOS Comput Biol* 14:e1005924, 2018
44. Aster RC, Borchers B, Thurber CH: *Parameter Estimation and Inverse Problems*. Waltham, MA, Elsevier Science, 2011
45. Sun N, Sun A: *Model Calibration and Parameter Estimation: For Environmental and Water Resource Systems*. Berlin, Germany, Springer-Verlag, 2015
46. Oden JT, Lima EABF, Almeida RC, et al: Toward predictive multiscale modeling of vascular tumor growth. *Arch Comput Methods Eng* 23:735-779, 2016
47. Akaike H: A new look at the statistical model identification. *Autom Control IEEE Trans* 19:716-723, 1974
48. Schwarz G: Estimating the dimension of a model. *Ann Stat* 6:461-464, 1978
49. Kucherenko S, Rodriguez-Fernandez M, Pantelides C, et al: Monte Carlo evaluation of derivative-based global sensitivity measures. *Reliab Eng Syst Saf* 94:1135-1148, 2009
50. Sobol' IM, Kucherenko S: A new derivative based importance criterion for groups of variables and its link with the global sensitivity indices. *Comput Phys Commun* 181:1212-1217, 2010
51. Bianca C, Chiacchio F, Pappalardo F, et al: Mathematical modeling of the immune system recognition to mammary carcinoma antigen. *BMC Bioinformatics* 13 (suppl 17):S21, 2012
52. Blower SM, Dowlatabadi H: Sensitivity and uncertainty analysis of complex models of disease transmission: An HIV model, as an example. *Int Stat Rev* 62:229-243, 1994
53. Jarrett AM, Cogan NG, Shirliff ME: Modelling the interaction between the host immune response, bacterial dynamics and inflammatory damage in comparison with immunomodulation and vaccination experiments. *Math Med Biol* 32:285-306, 2015
54. Cukier RI, Fortuin CM, Shuler KE, et al: Study of the sensitivity of coupled reaction systems to uncertainties in rate coefficients. I theory. *J Chem Phys* 59:3873-3878, 1973
55. Sobol' IM: Sensitivity estimates for nonlinear mathematical models. *Math Model Comput Exp* 1:407-414, 1993
56. Sobol' IM: Global sensitivity indices for nonlinear mathematical models and their Monte Carlo estimates. *Math Comput Simul* 55:271-280, 2001
57. Jarrett AM, Liu Y, Cogan NG, et al: Global sensitivity analysis used to interpret biological experimental results. *J Math Biol* 71:151-170, 2015
58. Jarrett AM, Cogan NG, Hussaini MY: Combining two methods of global sensitivity analysis to investigate MRSA nasal carriage model. *Bull Math Biol* 79:2258-2272, 2017
59. Borgonovo E: A new uncertainty importance measure. *Reliab Eng Syst Saf* 92:771-784, 2007
60. Liu Q, Homma T: A new computational method of a moment-independent uncertainty importance measure. *Reliab Eng Syst Saf* 94:1205-1211, 2009
61. Najm HN: Uncertainty quantification and polynomial chaos techniques in computational fluid dynamics. *Annu Rev Fluid Mech* 41:35-52, 2008
62. Lima EABF, Almeida RC, Oden JT: Analysis and numerical solution of stochastic phase-field models of tumor growth. *Numer Methods Partial Differ Equ* 31:552-574, 2015
63. Jaynes E: *Probability Theory: The Logic of Science*. New York, NY, Cambridge University Press, 2003
64. Hormuth DA II, Weis JA, Barnes SL, et al: Predicting in vivo glioma growth with the reaction diffusion equation constrained by quantitative magnetic resonance imaging data. *Phys Biol* 12:046006, 2015

65. Baldock AL, Rockne RC, Boone AD, et al: From patient-specific mathematical neuro-oncology to precision medicine. *Front Oncol* 3:62, 2013
66. Rockne RC, Trister AD, Jacobs J, et al: A patient-specific computational model of hypoxia-modulated radiation resistance in glioblastoma using 18F-FMISO-PET. *J R Soc Interface* 12:20141174, 2015
67. Hogeia C, Davatzikos C, Biros G: An image-driven parameter estimation problem for a reaction-diffusion glioma growth model with mass effects. *J Math Biol* 56:793-825, 2008
68. Konukoglu E, Clatz O, Menze BH, et al: Image guided personalization of reaction-diffusion type tumor growth models using modified anisotropic eikonal equations. *IEEE Trans Med Imaging* 29:77-95, 2010
69. Bondiau P-Y, Clatz O, Sermesant M, et al: Biocomputing: Numerical simulation of glioblastoma growth using diffusion tensor imaging. *Phys Med Biol* 53:879-893, 2008
70. Jbabdi S, Mandonnet E, Duffau H, et al: Simulation of anisotropic growth of low-grade gliomas using diffusion tensor imaging. *Magn Reson Med* 54:616-624, 2005
71. Hormuth DA 2nd, Weis JA, Barnes SL, et al: A mechanically coupled reaction-diffusion model that incorporates intra-tumoural heterogeneity to predict in vivo glioma growth. *J R Soc Interface* 14:20161010, 2017
72. Harpold HLP, Alvord ECJ Jr, Swanson KR: The evolution of mathematical modeling of glioma proliferation and invasion. *J Neuropathol Exp Neurol* 66:1-9, 2007
73. Wang CH, Rockhill JK, Mrugala M, et al: Prognostic significance of growth kinetics in newly diagnosed glioblastomas revealed by combining serial imaging with a novel biomathematical model. *Cancer Res* 69:9133-9140, 2009
74. Swan A, Hillen T, Bowman JC, et al: A patient-specific anisotropic diffusion model for brain tumour spread. *Bull Math Biol* 80:1259-1291, 2017
75. Mosayebi P, Cobzas D, Murtha A, et al: Tumor invasion margin on the Riemannian space of brain fibers. *Med Image Anal* 16:361-373, 2012
76. Clatz O, Sermesant M, Bondiau P-Y, et al: Realistic simulation of the 3-D growth of brain tumors in MR images coupling diffusion with biomechanical deformation. *IEEE Trans Med Imaging* 24:1334-1346, 2005
77. Hawkins-Daarud A, Rockne RC, Anderson ARA, et al: Modeling tumor-associated edema in gliomas during anti-angiogenic therapy and its impact on imageable tumor. *Front Oncol* 3:66, 2013
78. Hormuth D, Jarrett A, Feng X, et al: Angi-08. Predicting in vivo tumor growth and angiogenesis with an MRI calibrated biophysical model. *Neuro-oncology* 19:vi23-vi23, 2017
79. Atuegwu NC, Arlinghaus LR, Li X, et al: Integration of diffusion-weighted MRI data and a simple mathematical model to predict breast tumor cellularity during neoadjuvant chemotherapy. *Magn Reson Med* 66:1689-1696, 2011
80. Garg I, Miga MI: Preliminary investigation of the inhibitory effects of mechanical stress in tumor growth. *Proc SPIE* 6918:69182L, 2008
81. Weis JA, Miga MI, Yankeelov TE: Three-dimensional image-based mechanical modeling for predicting the response of breast cancer to neoadjuvant therapy. *Comput Methods Appl Mech Eng* 314:494-512, 2017
82. Jarrett AM, Hormuth DA, Barnes SL, et al: Incorporating drug delivery into an imaging-driven, mechanics-coupled reaction diffusion model for predicting the response of breast cancer to neoadjuvant chemotherapy: Theory and preliminary clinical results. *Phys Med Biol* 63:105015, 2018
83. Chen X, Summers R, Yao J: FEM-based 3-D tumor growth prediction for kidney tumor. *IEEE Trans Biomed Eng* 58:463-467, 2011
84. Mi H, Petitjean C, Dubray B, et al: Prediction of lung tumor evolution during radiotherapy in individual patients with PET. *IEEE Trans Med Imaging* 33:995-1003, 2014
85. Liu Y, Sadowski SM, Weisbrod AB, et al: Patient specific tumor growth prediction using multimodal images. *Med Image Anal* 18:555-566, 2014
86. Chen X, Summers RM, Yao J: Kidney tumor growth prediction by coupling reaction-diffusion and biomechanical model. *IEEE Trans Biomed Eng* 60:169-173, 2013
87. Mi H, Petitjean C, Vera P, et al: Joint tumor growth prediction and tumor segmentation on therapeutic follow-up PET images. *Med Image Anal* 23:84-91, 2015

